Supporting Information

Porous aromatic frameworks-based sequential therapeutic strategy for the treatment of periodontitis

Fuming Yang [a,b], Enpeng Xi [b], Yun Zhao [b], Gang Wang [*a], Nan Gao [**b], and Guangshan Zhu [b]

[a] *China-Japan Union Hospital of Jilin University, Changchun 130033, China*
[b] *Key Laboratory of Polyoxometalate and Reticular Material Chemistry of Ministry of Education and Faculty of Chemistry, Northeast Normal University, Changchun 130024, China*

[a] Corresponding author at China-Japan Union Hospital of Jilin University, Changchun 130033, China.
[b] Corresponding author at: Key Laboratory of Polyoxometalate and Reticular Material Chemistry of Ministry of Education and Faculty of Chemistry, Northeast Normal University, Changchun 130024, China.
E-mail addresses: Gang Wang, w_g@jlu.edu.cn; Nan Gao, gaon320@nenu.edu.cn.

Supporting Information

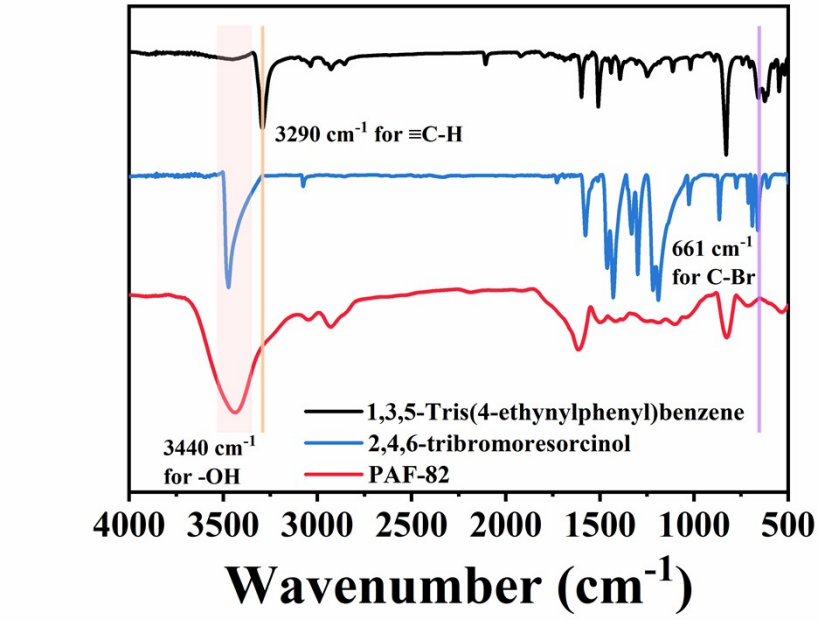

Figure S1 FTIR images of 1,3,5-Tris(4-ethynylphenyl)benzene, 2,4,6-tribromoresorcinol and PAF.

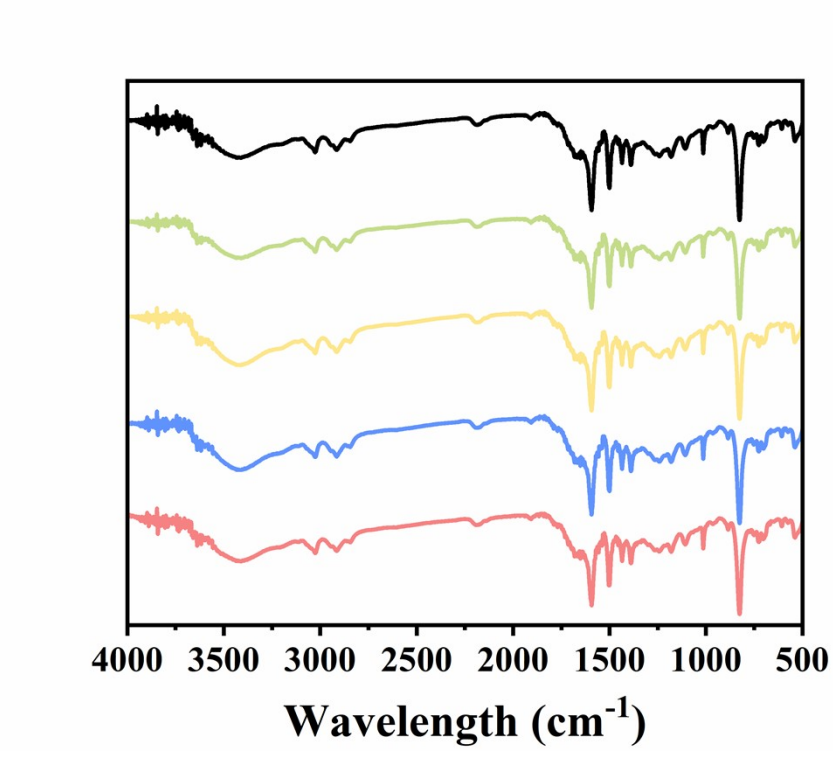

Figure S2 FTIR images of PAF after being soaked for 7 days in different environments (Black: nothing; Green: ethanol; Yellow: 1 M NaOH; Blue: 1 M HCl; Red: 1× PBS).

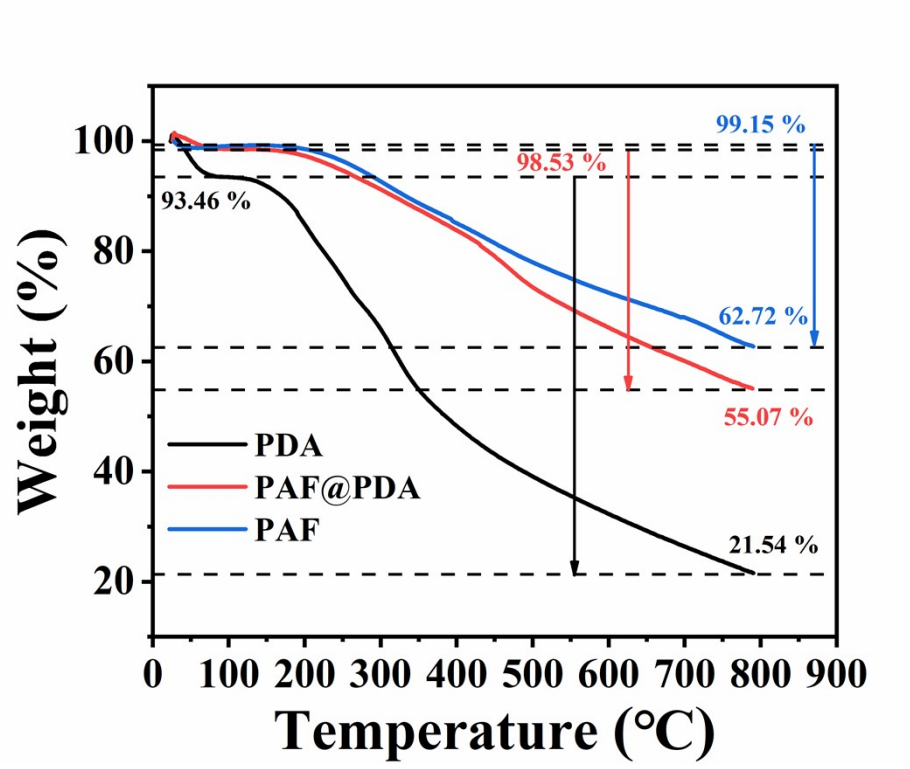

Figure S3 TGA images of PDA, PAF and PAF@PDA.

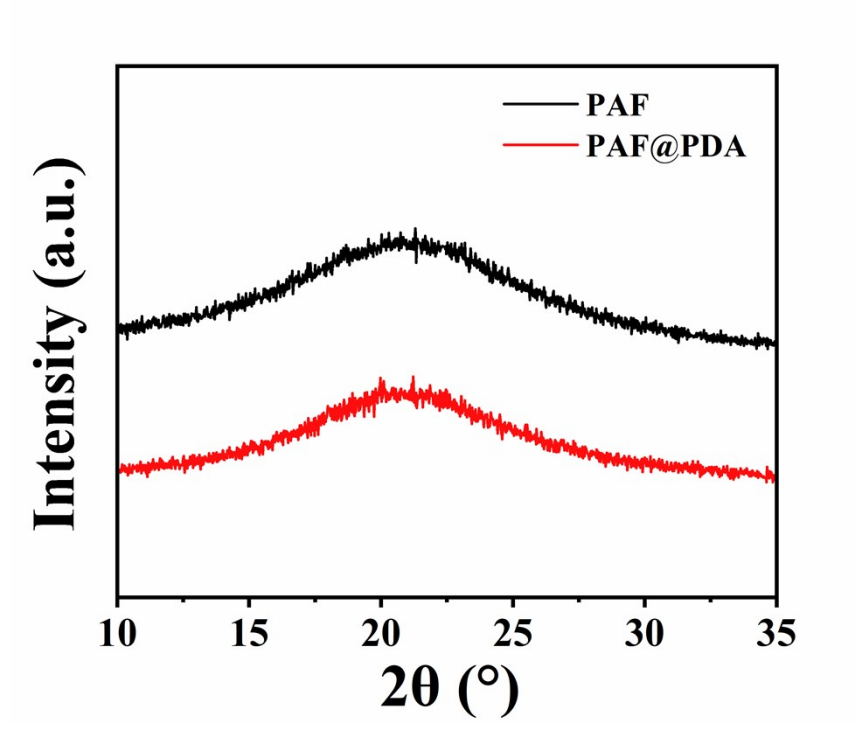

Figure S4 XRD images of PAF and PAF@PDA.

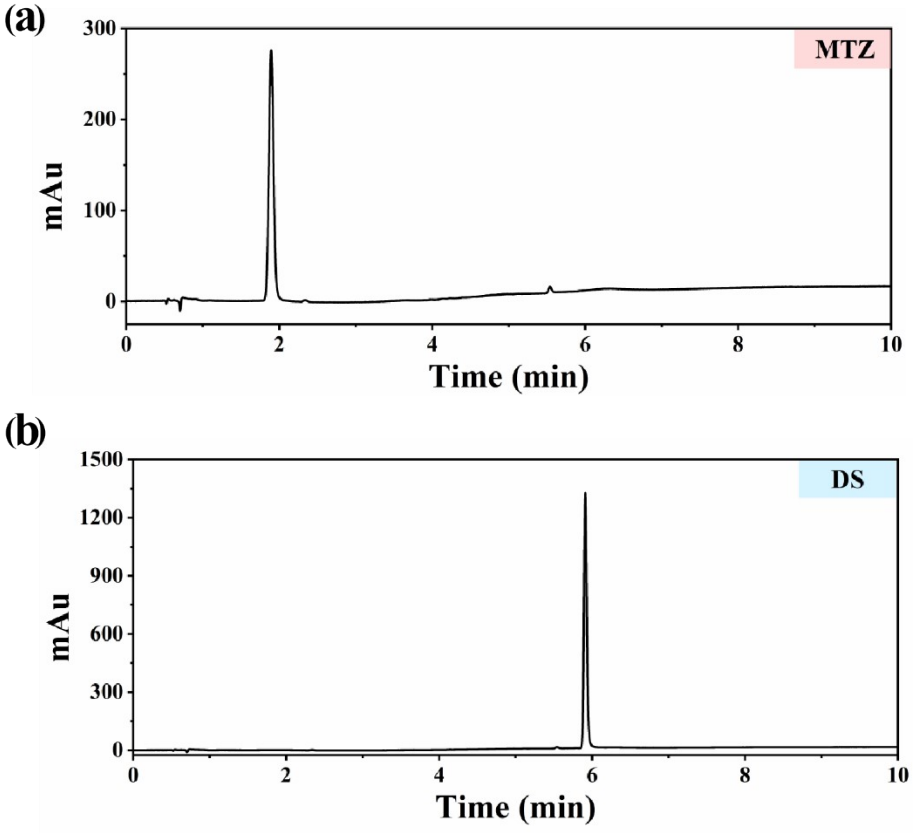

Figure S5 HPLC determination of MTZ and DS. (a) HPLC image of MTZ at a concentration of 1 mg/mL. (b) HPLC image of DS at a concentration of 1 mg/mL.

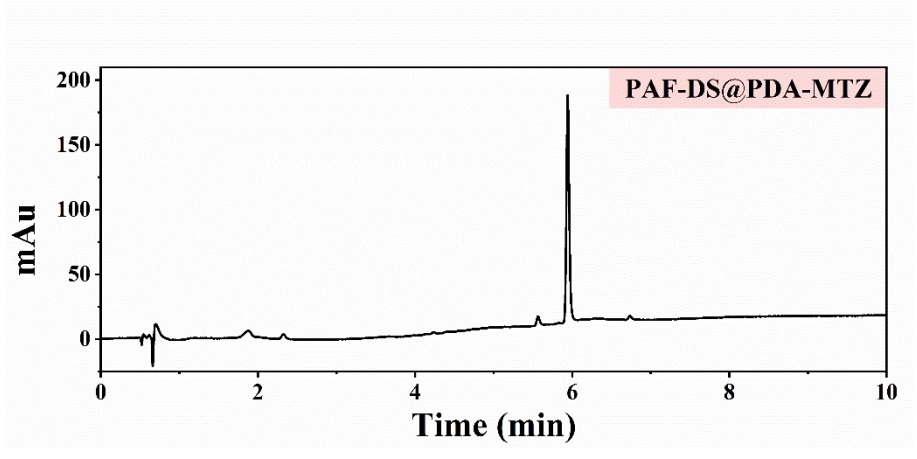

Figure S6 HPLC image of PAF-DS@PDA-MTZ in the supernatant.

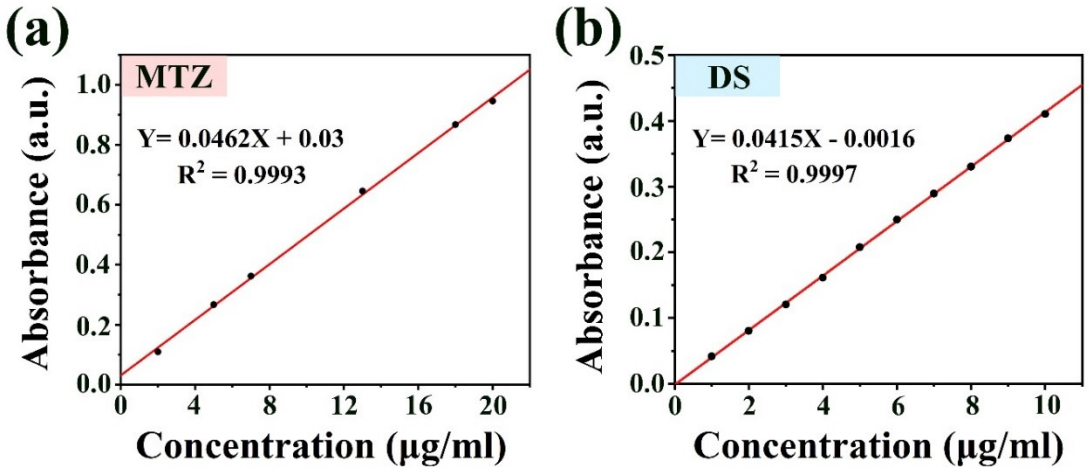

Figure S7 Standard curves for UV-vis determination of MTZ and DS. (a) Standard curve for MTZ. (b) Standard curve for DS.

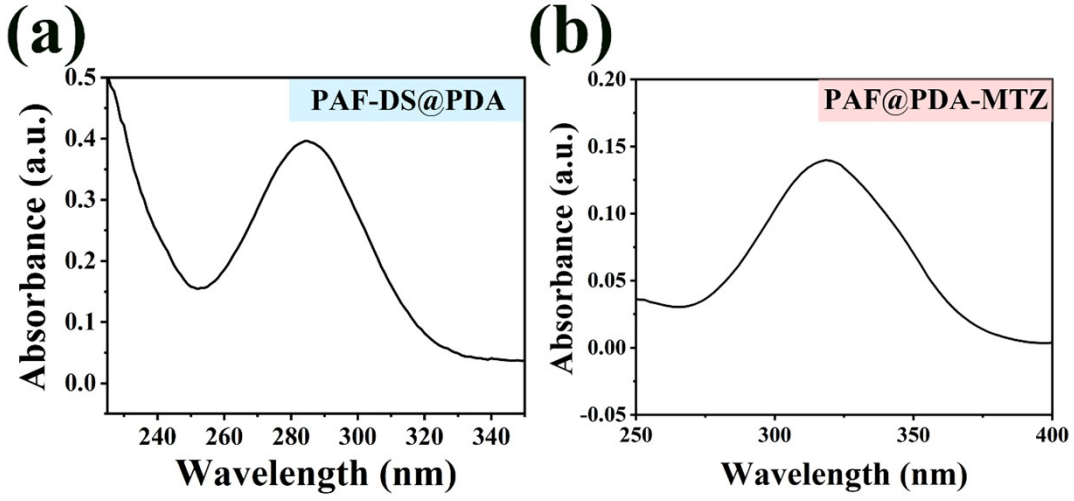

Figure S8 UV-vis determination of DS and MTZ in PAF-DS@PDA and PAF@PDA-MTZ supernatants. (a) UV-vis image of DS in PAF-DS@PDA supernatant (Diluted 10 times). (b) UV-vis image of MTZ in PAF@PDA-MTZ supernatant (Diluted 10 times).

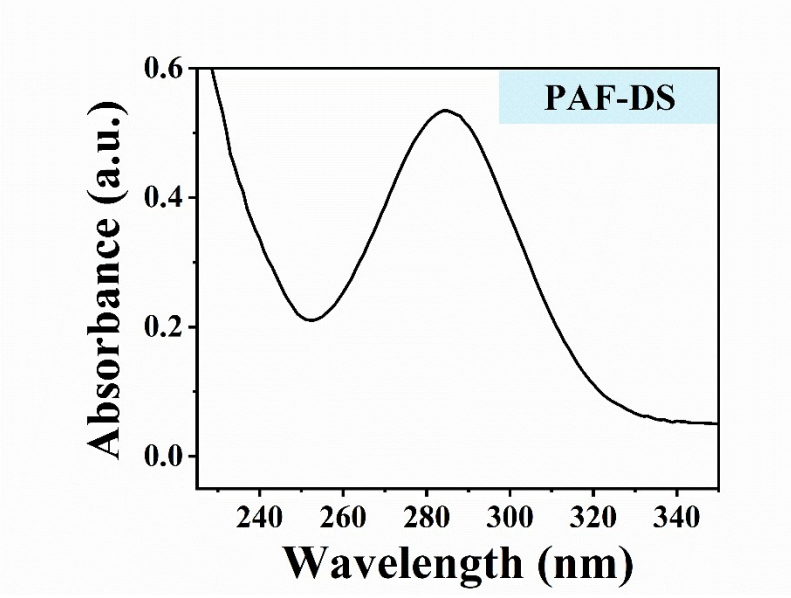

Figure S9 UV-vis image of DS in PAF-DS supernatant (Diluted 10 times).

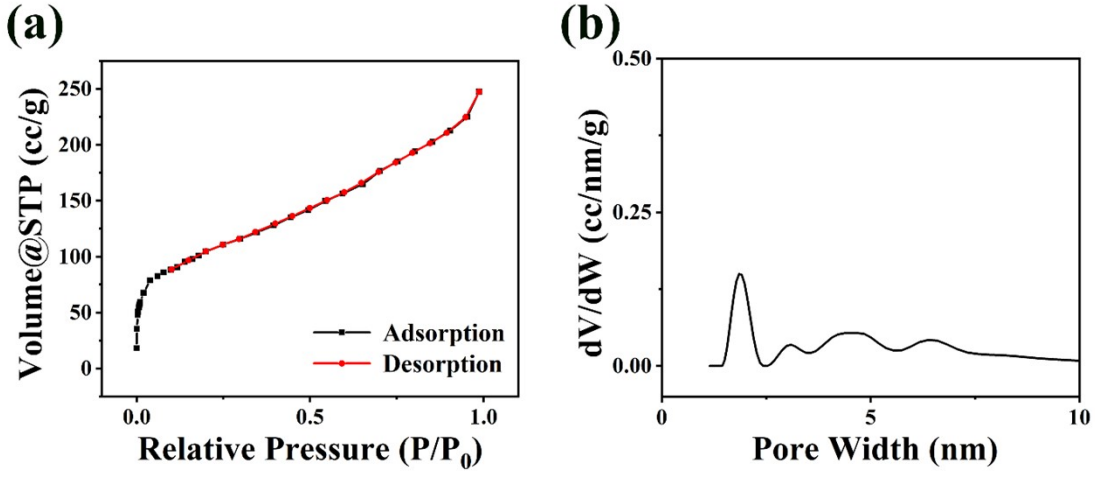

Figure S10 (a) N_2 adsorption-desorption isotherm of PAF-DS. (b) Pore size distribution of PAF-DS.

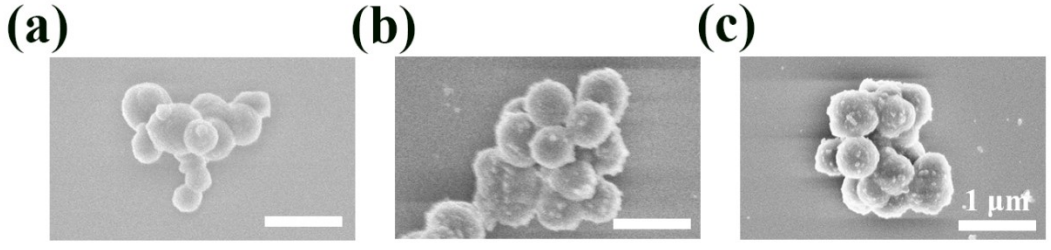

Figure S11 SEM images of (a) PAF-DS, (b) PAF-DS@PDA and (c) PAF@PDA-MTZ.

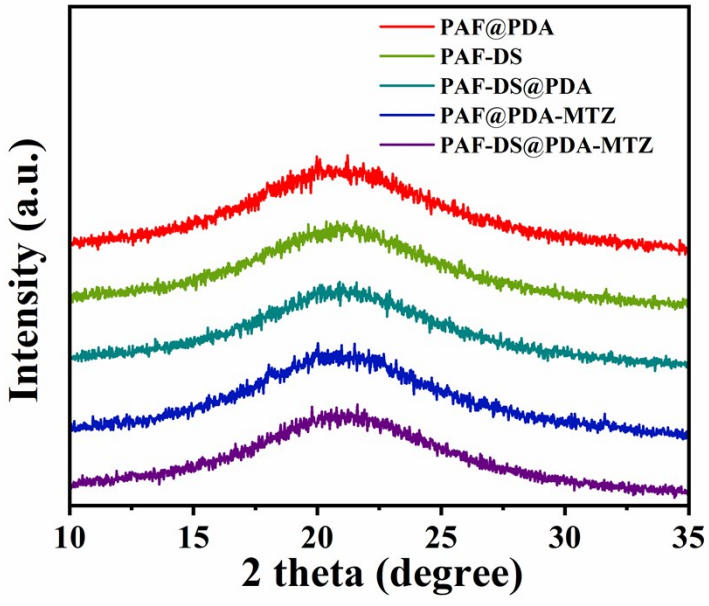

Figure S12 XRD images of PAF@PDA, PAF-DS, PAF-DS@PDA, PAF@PDA-MTZ and PAF-DS@PDA-MTZ.

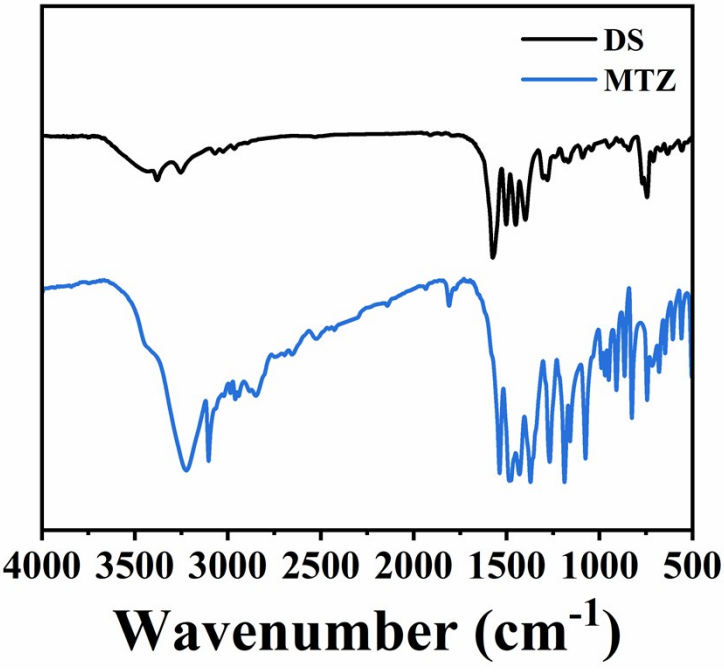

Figure S13 FTIR images of DS and MTZ.

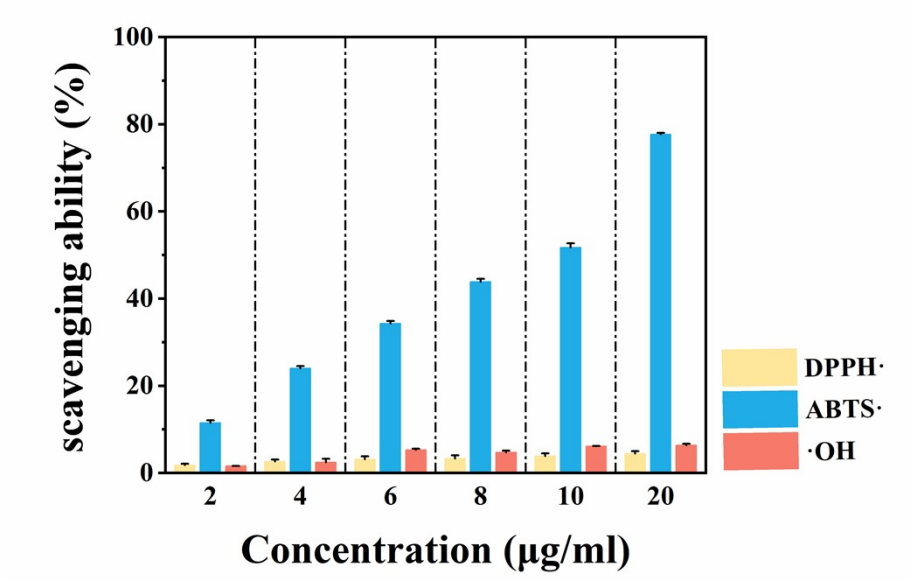

Figure S14 Determination of antioxidant capacity of different concentrations of DS by DPPH method, ABTS method and Fenton reaction method.

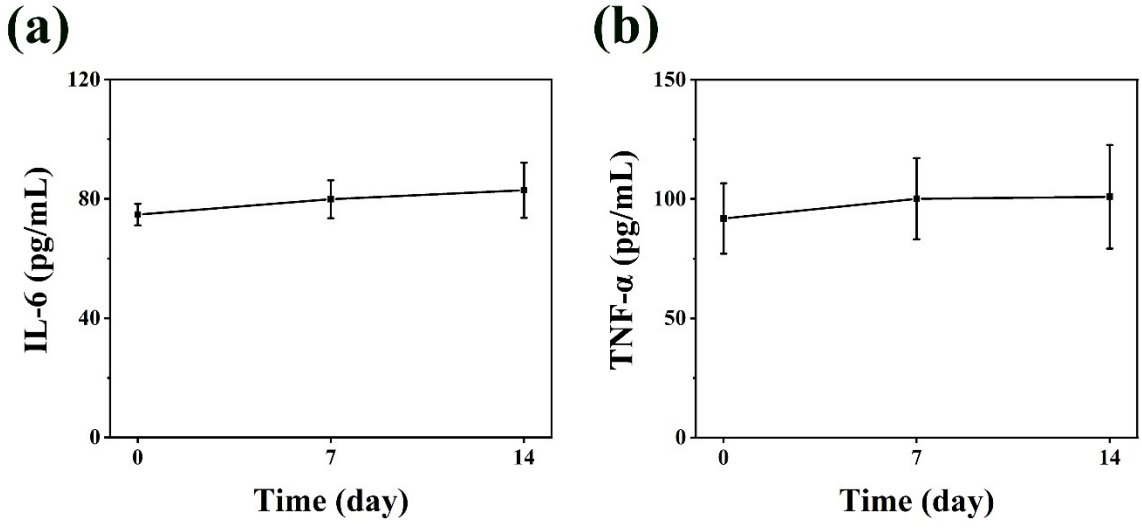

Figure S15 Images of (a) IL-6 level and (b) TNF-α level in the biosafety experiment.

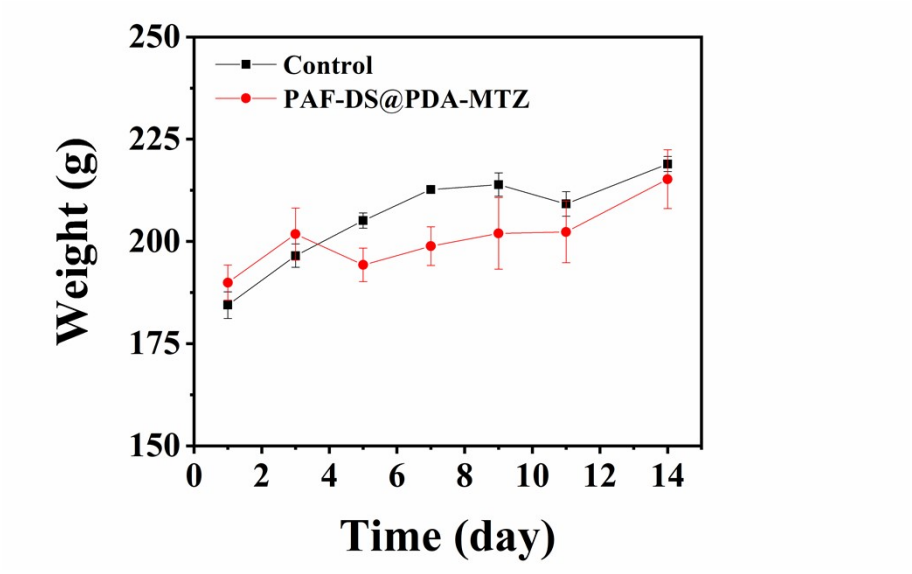

Figure S16 Image of body weight changes in the biosafety experiment.

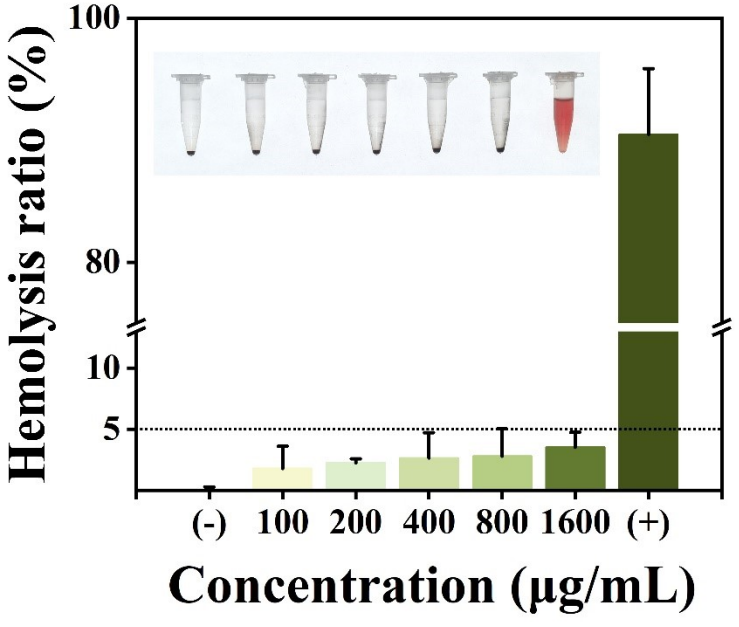

Figure S17 Hemolysis ratio of RBCs treated with different concentrations of PAF-DS@PDA-MTZ.

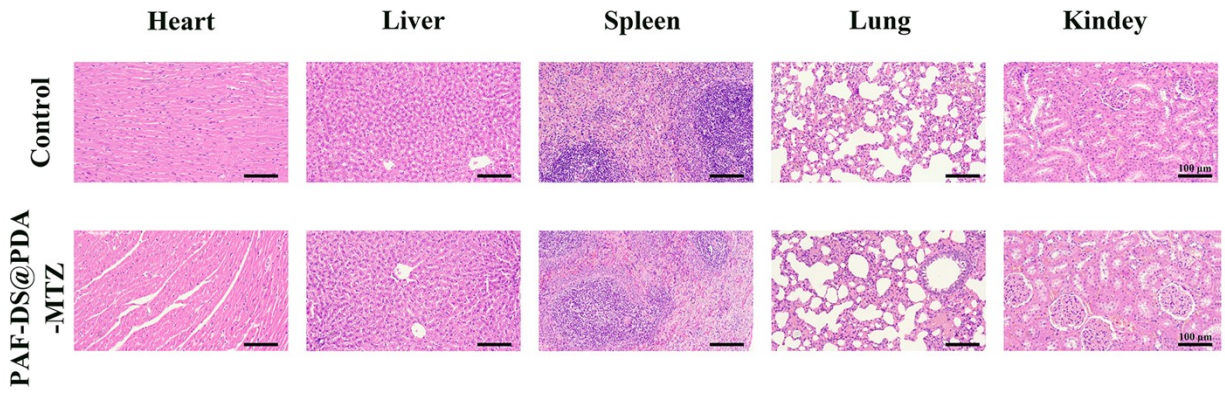

Figure S18 H&E staining of major organs for biosafety experiments (scale bars are 100 μm).

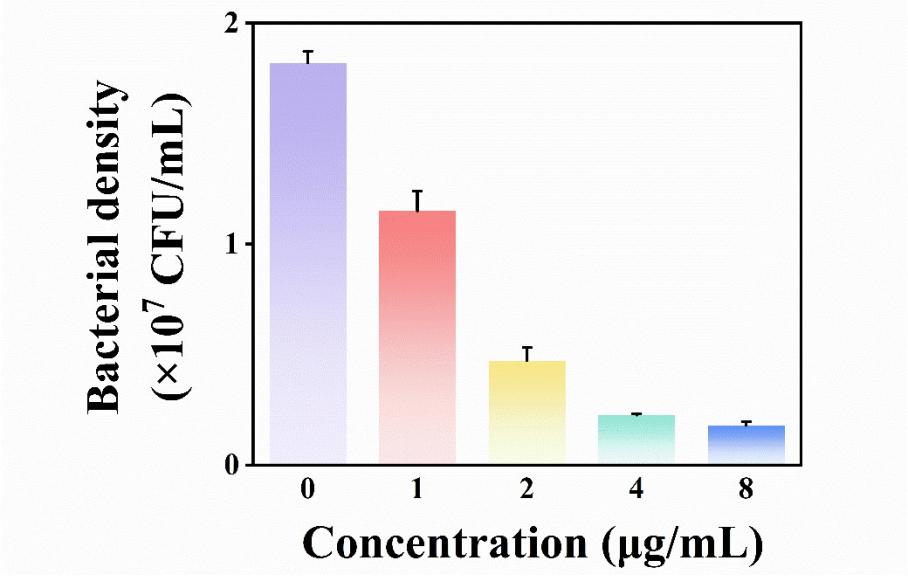

Figure S19 Determination of the bactericidal effect of different concentrations of MTZ on Porphyromonas gingivalis at 5 hours.

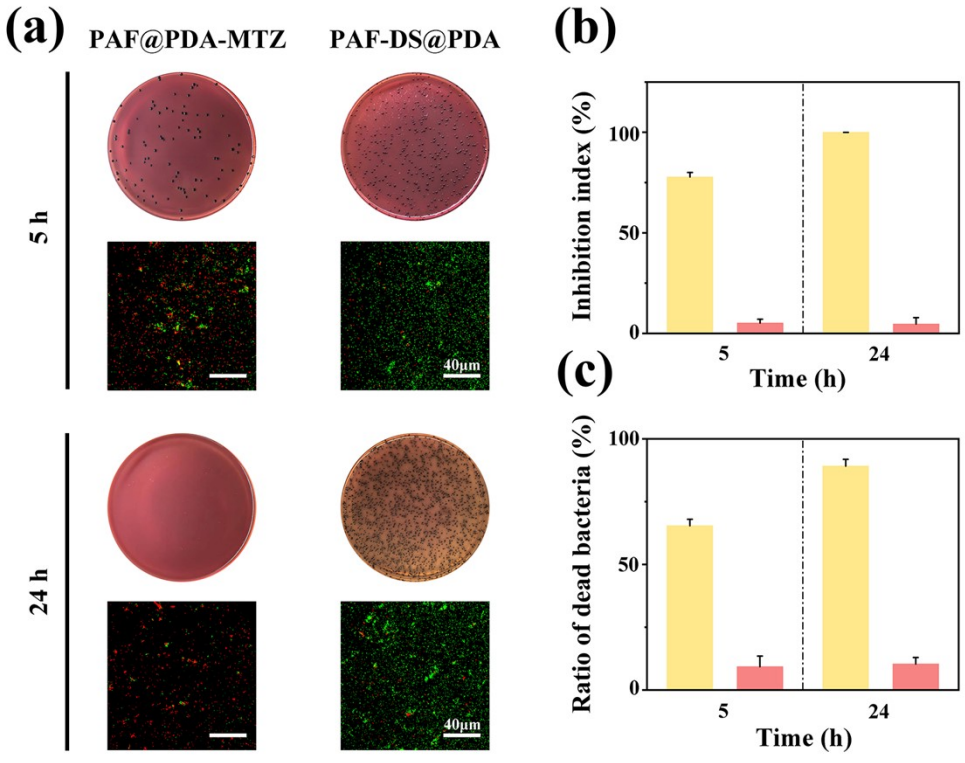

Figure S20 Characterization of the P. g-killing ability. (a) Colony-forming assay and Live/dead staining of P. g after treatment with PAF@PDA-MTZ, PAF-DS@PDA (at equivalent drug concentrations), respectively. (b) Quantification of colony-forming assay of P. g after treatment. (c) Quantification of Live/dead staining of P. g after treatment.

Figure S21 Injectability of PAF-DS@PDA-MTZ-Gel through the syringe.

Figure S22 Macroscopic self-healing property of PAF-DS@PDA-MTZ-Gel.

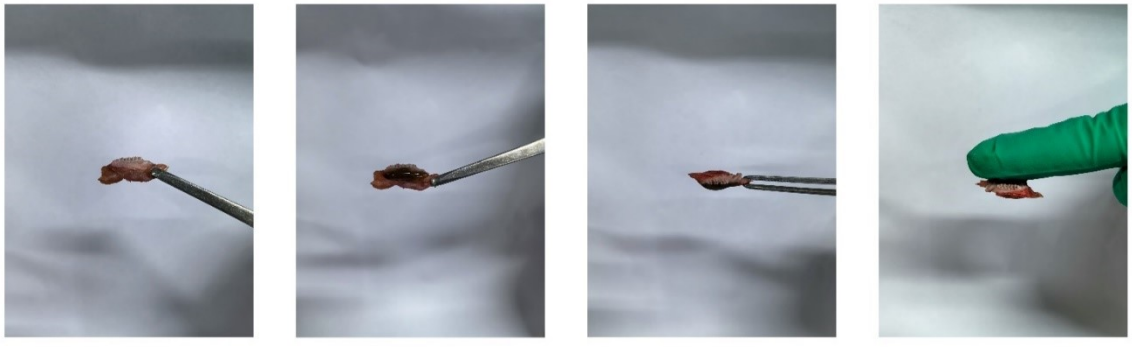

Figure S23 Adhesion to rat gingiva.

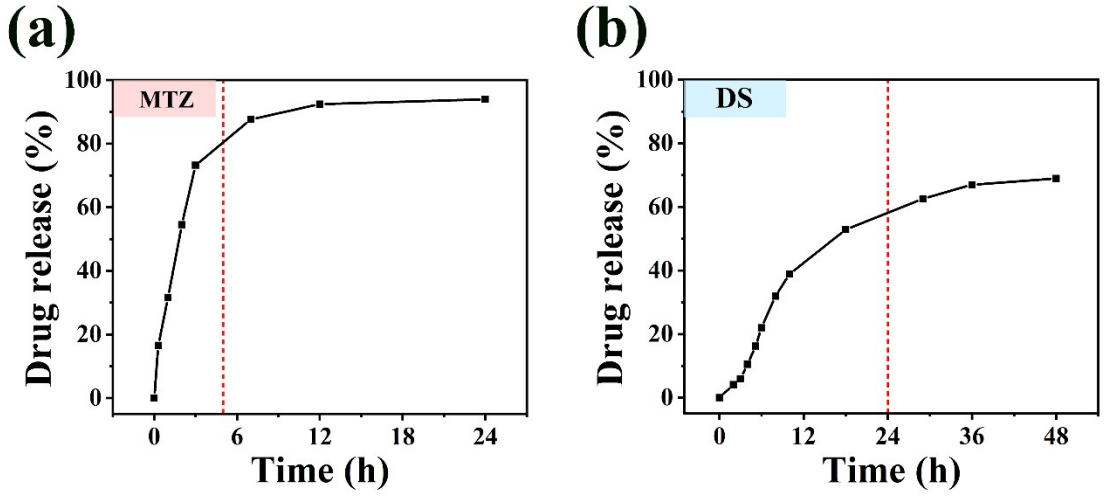

Figure S24 Release process of MTZ and DS from the PAF@PDA-Gel loaded with MTZ or DS.

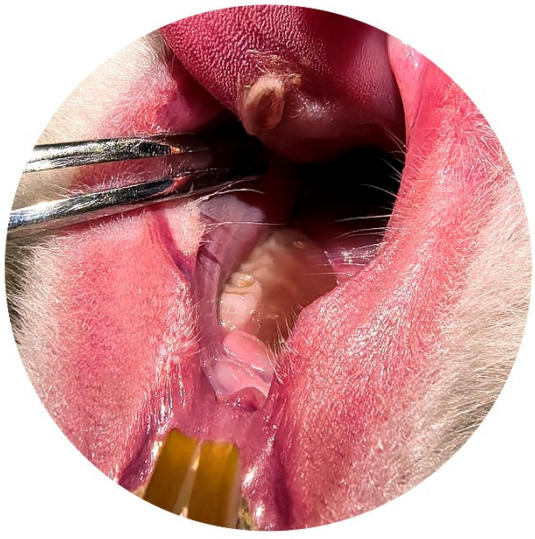

Figure S25 Image of 200 μL PAF-DS@PDA-MTZ-Gel adhered to periodontal tissue for treatment.

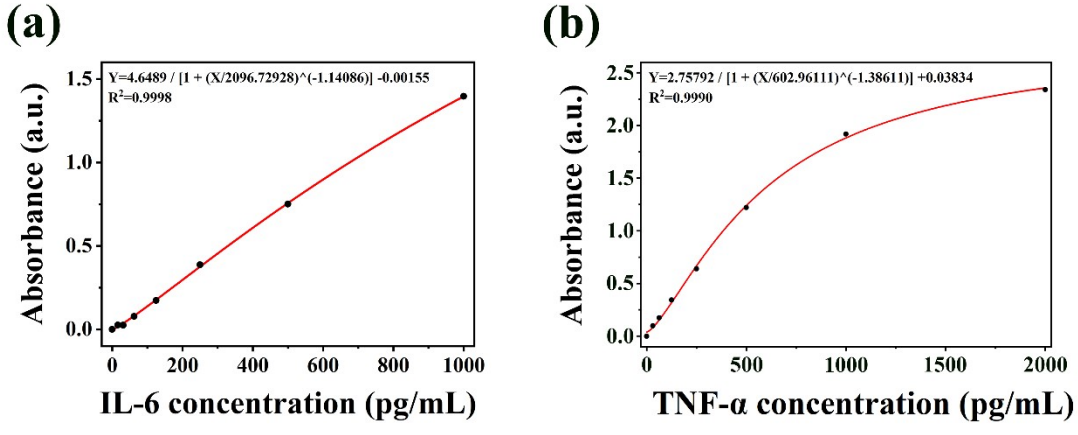

Figure S26 Standardized curves for (a) IL-6 and (b) TNF-α.

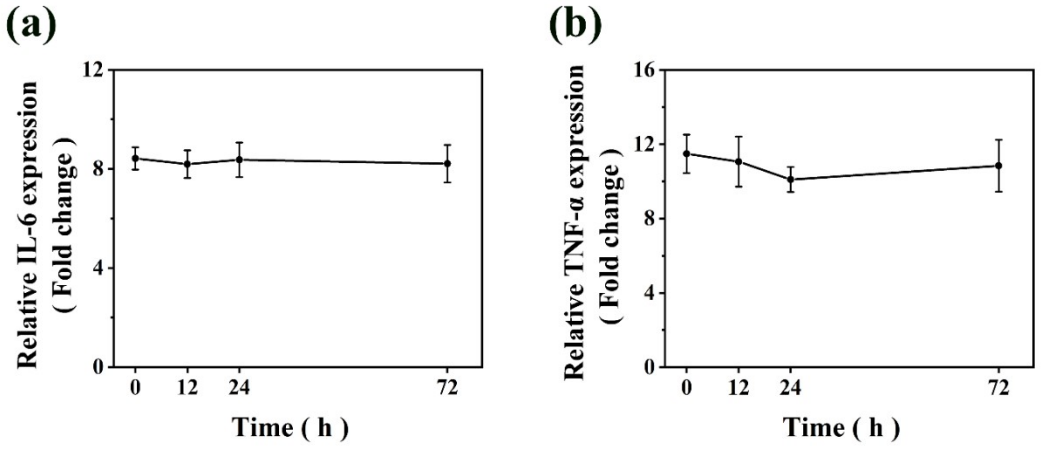

Figure S27 Images of (a) IL-6 level and (b) TNF-α level in Blank-Gel group of the biosafety experiment.

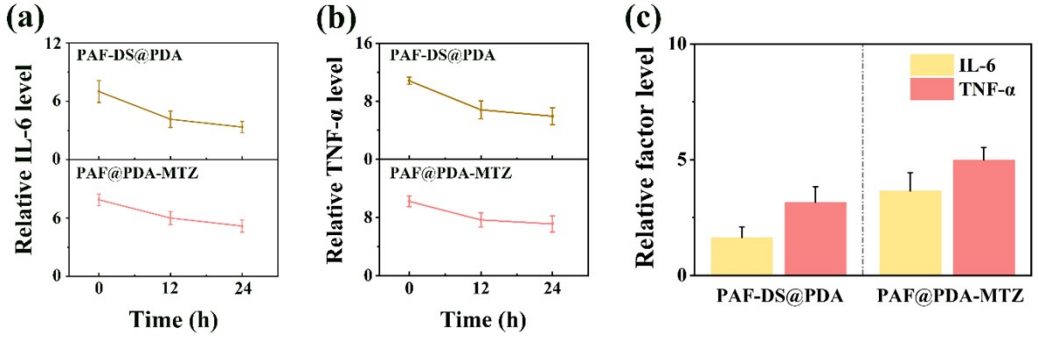

Figure S28 Images of (a) IL-6 levels and (b) TNF-α levels in each group of the biosafety experiment. (c) Comparative images of inflammatory factor levels in the groups at 72 h.

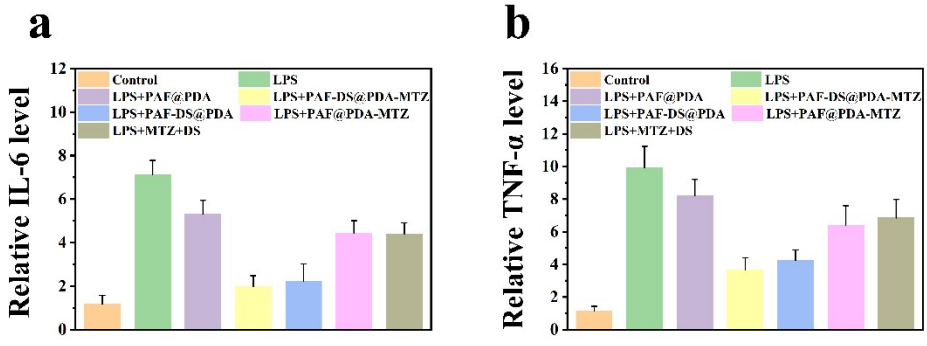

Figure S29. Comparative images of (a) IL-6 levels and (b) TNF-α levels in the groups at 48 h.

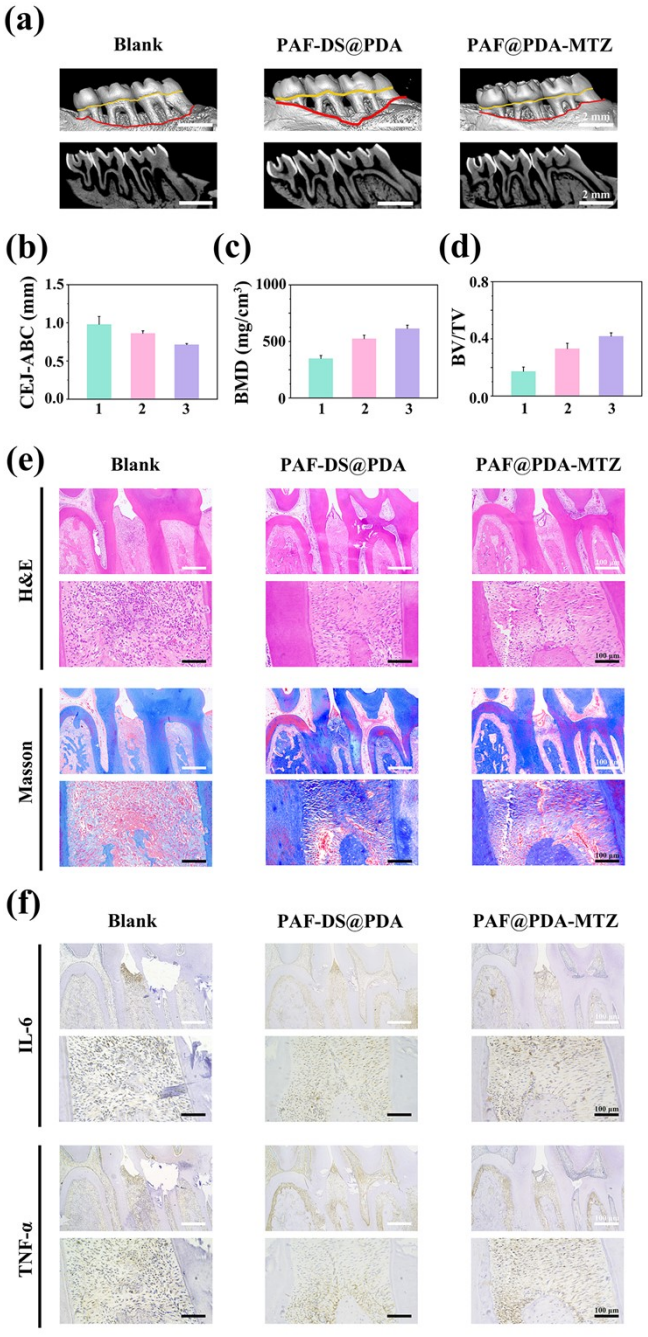

Figure S30 (a) 3D reconstructed and the buccopalatal section images of the maxillary molars with different treatments by Micro-CT. Red and yellow lines represent the distance between ABC and CEJ (scale bar = 2 mm). (b) Quantitative evaluation of the distance between ABC and CEJ. (c-d) The quantitative statistics of different parameters of the alveolar bone (1: Blank; 2: PAF-DS@PDA; 3: PAF@PDA-MTZ). (e) H&E staining and Masson staining images of the periodontal tissue. (f) Immunohistochemical staining of periodontal tissue for IL-6 and TNF-α (white scale bar = 500 μm, black scale bar = 100 μm). Data are means ± s.d. (n = 5). $*p < 0.05$, $**p < 0.01$, $***p < 0.001$.

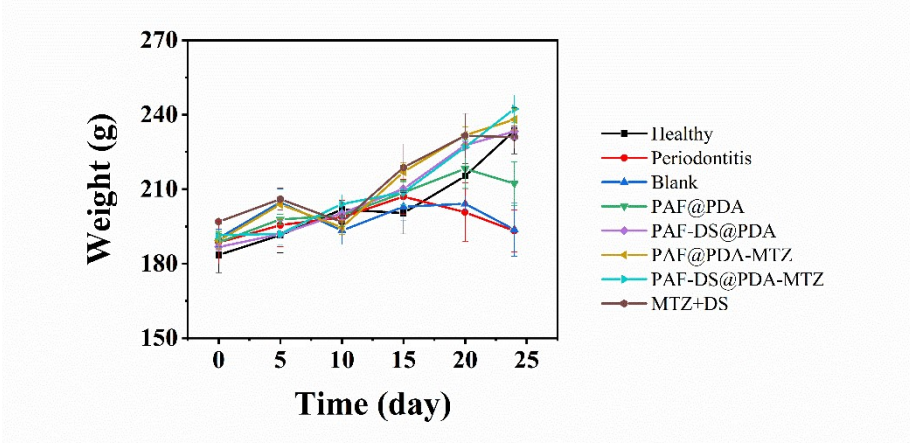

Figure S31 Changes in body weight of rats.

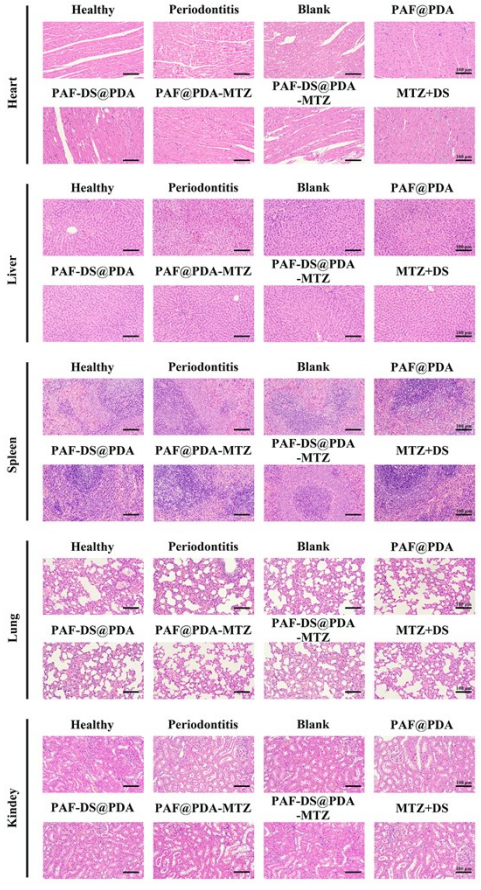

Figure S32 H&E staining of major organs (scale bar: 100 μm).